Auxiliary Materials

"Low frequency signals in tree-ring stable isotopes"
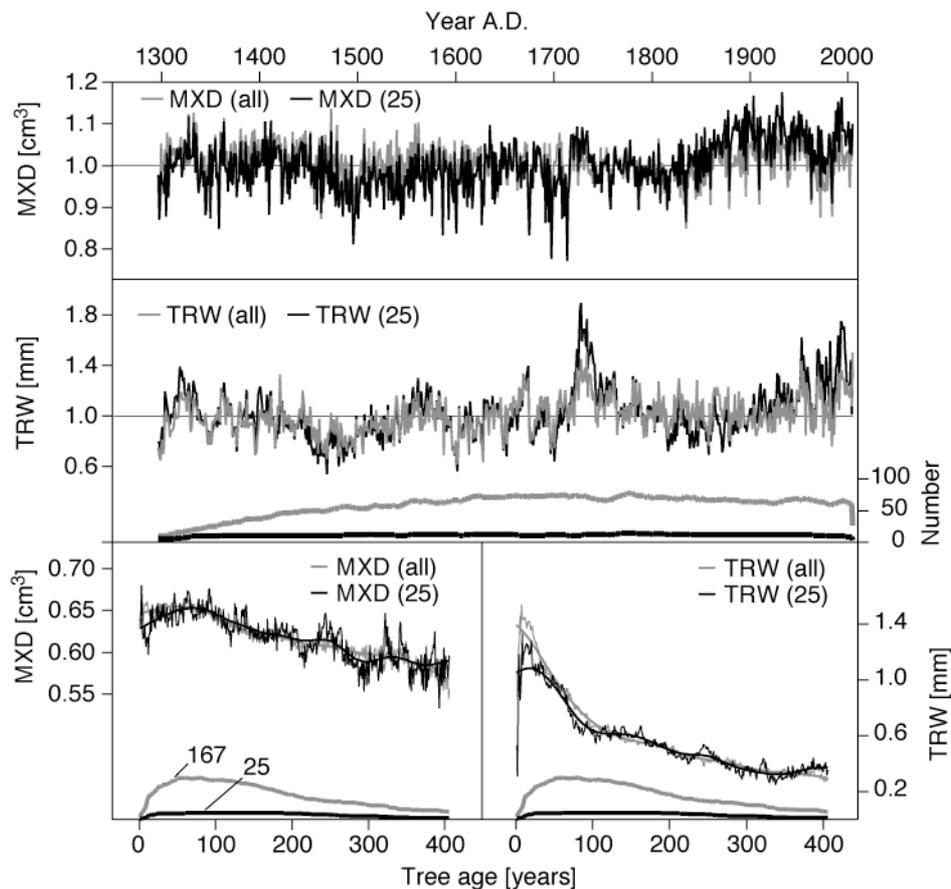
by

Jan Esper, David C. Frank, Giovanna Battipaglia, Ulf Büntgen,
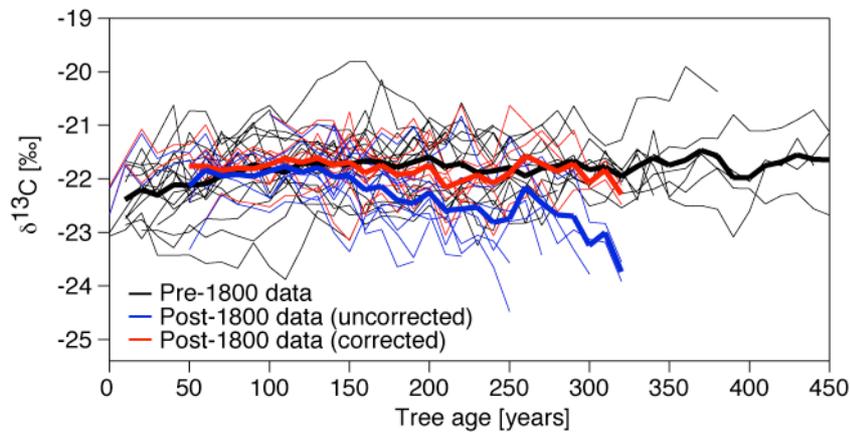Christopher Holert, Kerstin Treydte, Rolf Siegwolf, Matthias Saurer

Tree-Ring Data

The 25 pine trees used for stable isotope analysis are part of a larger collection of 203 samples from which MXD and TRW data have been measured [Büntgen et al., 2008]. To estimate the effect of sub-sampling, a comparison of the RCS-detrended chronologies and the age-aligned data is shown for MXD and TRW (Figure A1). This assessment reveals strong coherence between RCS chronologies (r = 0.80 for MXD and 0.84 for TRW over the 1300-2005 period), with obvious deviations limited to the late 19th (MXD) and early 18th centuries (TRW). Also the age-aligned data appear quite similar, except the less replicated subset mean is more variable. Substantial deviations are limited to the first decades after germination in both MXD and TRW, when sample replication, due to pith offset (PO), is low. Young tree-rings of the 25-tree subset indicate lower growth rates over the first ~30 years.

Figure A1. Comparison of the 25 samples used for isotope measurements with all tree-ring data from site Gerber in the Spanish Pyrenees. Upper and middle panels show RCS detrended MXD and TRW chronologies. Grey curves are chronologies averaging all 203 Gerber tree samples from which MXD data are available [see Büntgen et al., 2008]; black curves are chronologies averaging the 25 trees used for isotope measurements. Bold curves (bottom of middle panel) show the replication of the full and subset data. Bottom panel shows the same MXD and TRW data after alignment by cambial age. Thin curves are arithmetic means, bold curves 100-year splines, and bottom curves replication.

Atmospheric Correction

To remove trend related to changes in the isotopic composition of the atmosphere, the so-called Suess Effect [Suess, 1955], a correction factor that monotonically increases from 0‰ in A.D. 1800 to 1.6‰ in 2000, derived from ice core and recent atmospheric data, is applied to the tree-ring $\delta^{13}C$ measurements [Leuenberger, 2007]. To illustrate the effect of this correction, the $\delta^{13}C$ data are split into pre- and post-1800 measurements – after truncation of some data bridging over the A.D. 1800 date line – and aligned by biological age (Figure A2). Removal of the Suess Effect adjusts the uncorrected data (the blue curve) to the level of the pre-1800 data, suggesting that consideration of the diluted atmospheric carbon concentrations alone is sufficient to remove non-climatic trends from the tree-ring $\delta^{13}C$ data [see Treydte et al., 2009 for a discussion of other correction factors].

Figure A2. $\delta^{13}C$ correction. A comparison of pre-1800 (in black) versus post-1800 (blue and red) carbon data is shown. Post-1800 measurements are differentiated into uncorrected and corrected timeseries, emphasizing the adjustment due to fossil carbon burning and changes in the isotopic composition of the atmosphere. All timeseries are aligned by tree age considering pith offset and data truncation (see text). Thin curves represent decadal data from individual trees (16 pre-1800, 9 post-1800), bold curves are arithmetic means calculated over periods with >2 trees.
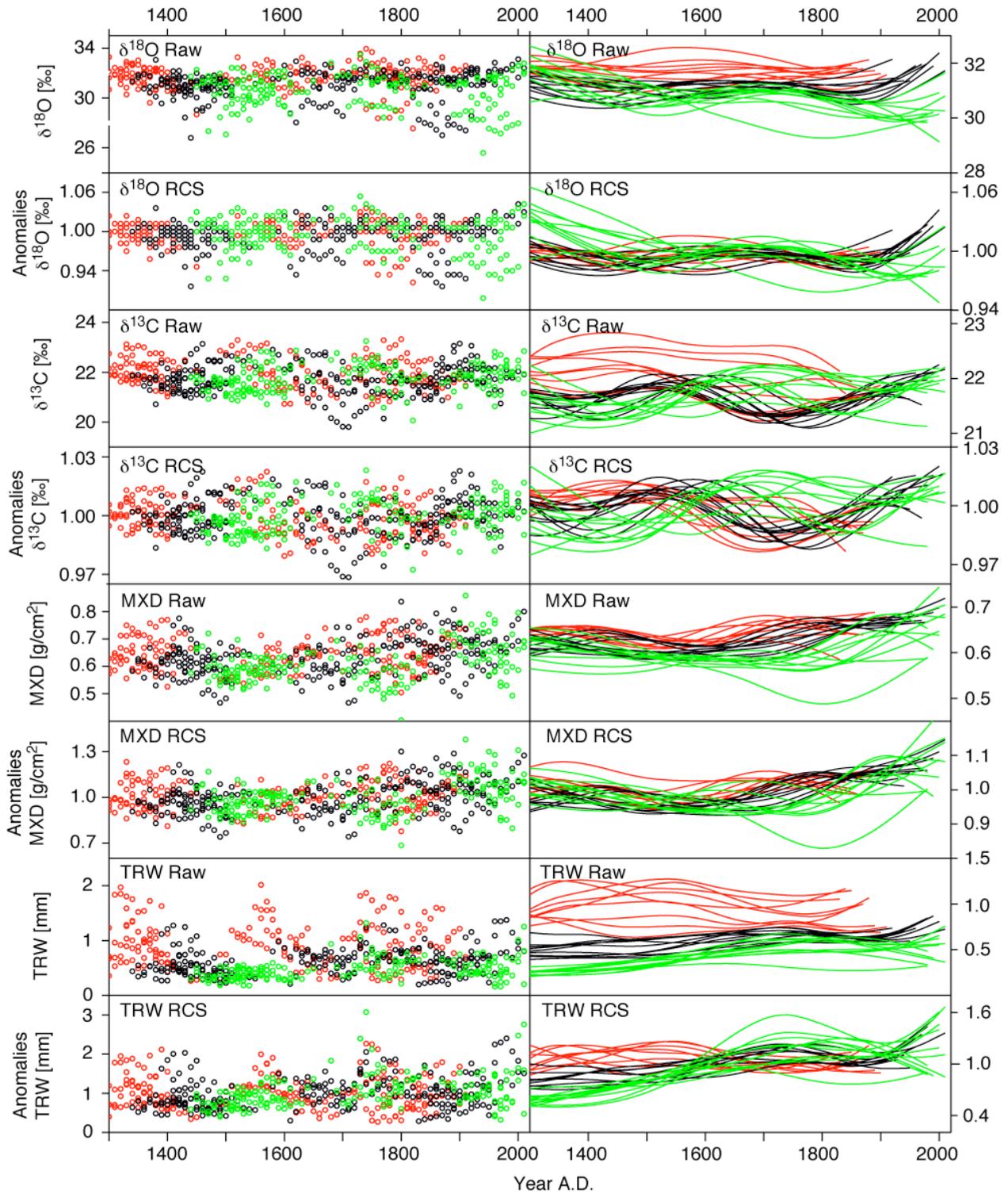
Age-Class Decomposition

The decomposition of data into age-classes and application of gap-bridging splines allows an assessment of time-dependent age trends in tree-ring parameters. Figure A3 illustrates how *(i)* young (<100 years) middle (100-200 years) and old (>200 years) data points are clustered over the last 700 years, *(ii)* the values of young (raw) data are generally larger than the middle and old data, particularly for δ^{18}O and TRW, *(iii)* these differences are captured by 30-year smoothing splines, and *(iv)* the ranking from young (≈ large values) to old (≈ small values) data points is removed by RCS detrending. The splines fitted to the raw data range:

for δ^{18}O from 29.3‰ around 1800 (at an age of 300) to 32.6‰ in the 16th century (age 50),

for δ^{13}C from 21.2‰ in the 14th century (age 300) to 22.7‰ in the 15th century (age 20),

for MXD from 0.49 g/cm^3 around 1800 (age 290) to 0.69 g/cm^3 in the 19th century (age 70),
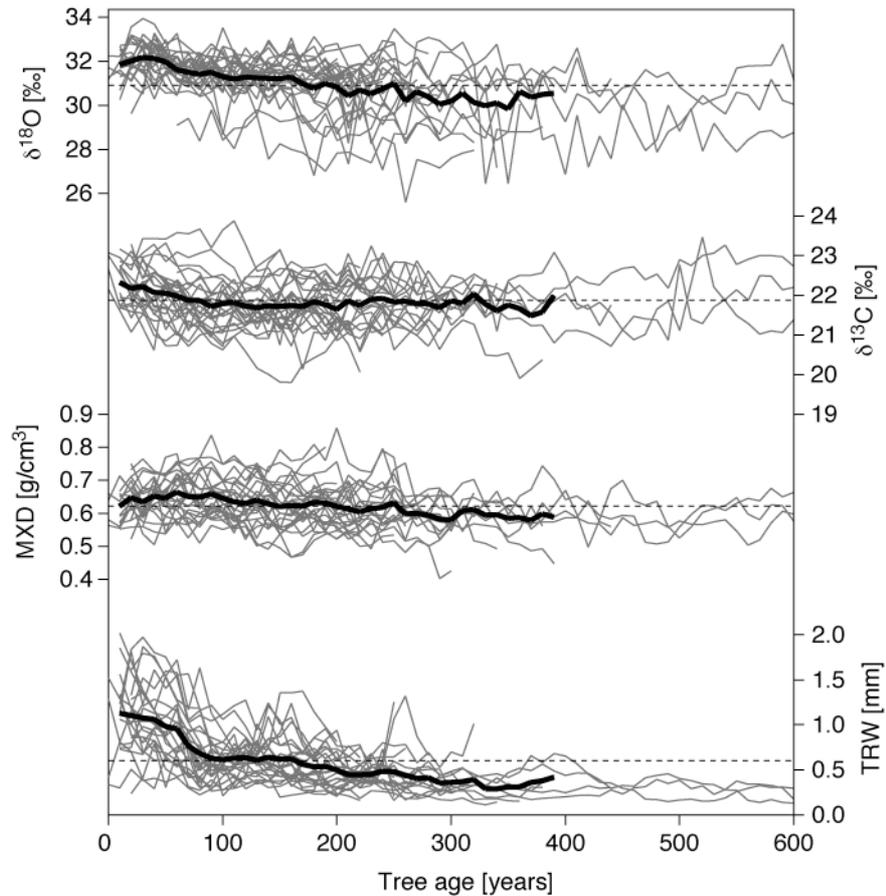
for TRW from 0.2 mm in the 14th century (age 270) to 1.3 mm in the 15th century (age 40).

Figure A3. Effects of age trend removal. Circles in left column panels are the single $\delta^{18}O$, $\delta^{13}C$, MXD, and TRW data points. Red circles represent data points ranging from 20 to 100 years biological age (replication of the 10-year class <5 trees), black circles from 110 to 200 years, and green circles from 210 to 300 years (again replication above 300 years is <5 trees). For each parameter, $\delta^{18}O$, $\delta^{13}C$, MXD, and TRW, the raw and RCS-detrended data are shown. Right hand panels show 30-year splines fit to the single age class data points; red curves for age classes 20, 30, ..., 100 years; black curves for 110, 120, ..., 200 years, and green curves for 210, 220, ..., 300 years. No splines were fit to age classes <20 and >300 as too few data points are available.
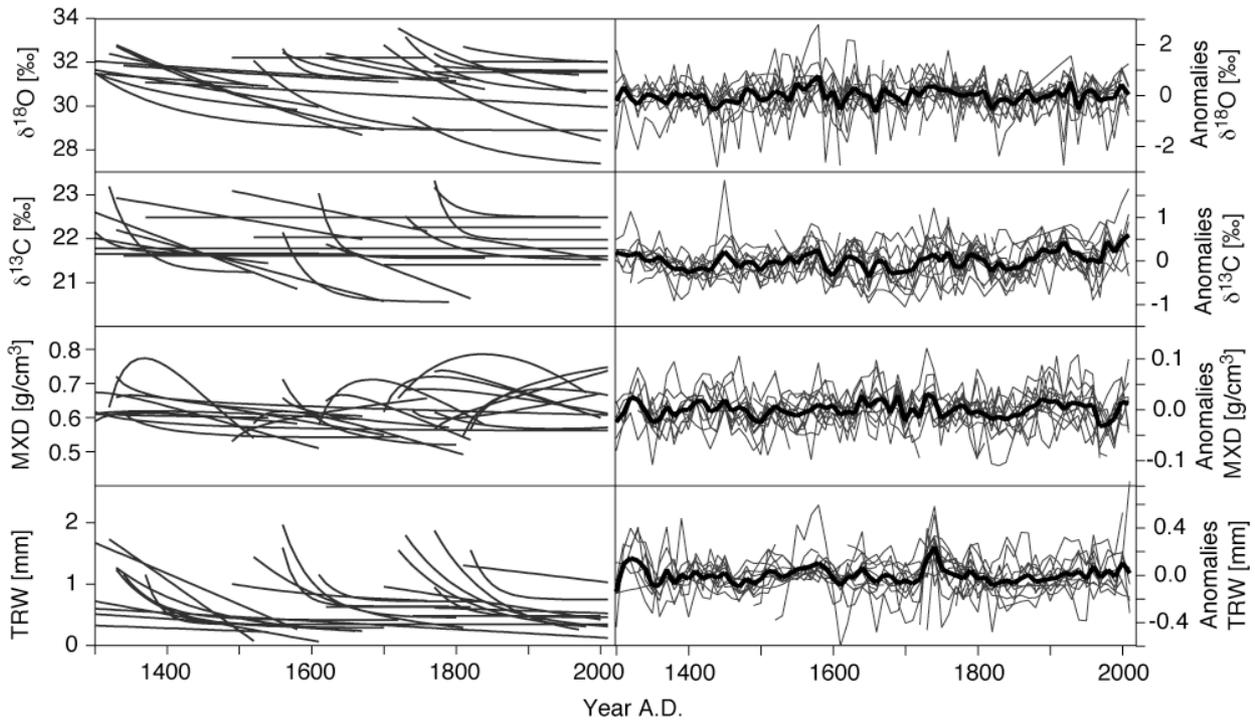
Data Alignment

Alignment of the individual measurement series emphasizes the association between the various tree-ring parameters and age. A number of records shown in figure A4 are, however, not exactly aligned to zero, as the corresponding core samples did not contain the pith. These data were shifted along the x-axis in accordance with PO (see Methods) estimated for each of the 25 trees. PO of the Pyrenees pine data ranges from 0-60 years, with an average of 14 years.

Figure A4. Age trend in δ^{18}O, δ^{13}C, MXD, and TRW data. Shown are the decadally resolved individual measurement series after alignment by tree age. Black curves are arithmetic means calculated over periods replicated by >4 trees. Dashed lines are mean values as in figure 1. δ^{13}C y-axis is inverted.
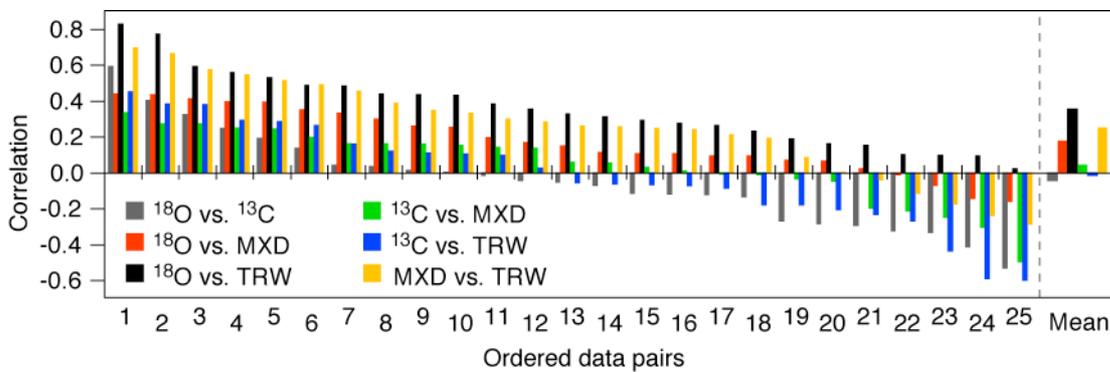
'Best-Fit' Detrending

Comparison of various detrending methods indicated NegExp (δ^{18}O, δ^{13}C, TRW) and Hug (MXD) to produce minimum squared residual chronologies. The individual NegExp and Hug, as well as straight-line fits chosen by Arstan [Cook, 1985], are shown in figure A5 (left column). Residual timeseries (right column) highlight the variance between detrended records. Individual detrending, using NegExp and Hug options in Arstan, removes low frequency variance from the data.

Figure A5. Detrending of tree-ring parameters. The individual growth curves fit to the original measurements (left column panels) and derived residuals (right column panels) are shown for δ^{18}O, δ^{13}C, MXD, and TRW. Fitted growth curves are NegExp and linear functions for the isotope parameters and TRW, and Hug functions for MXD.
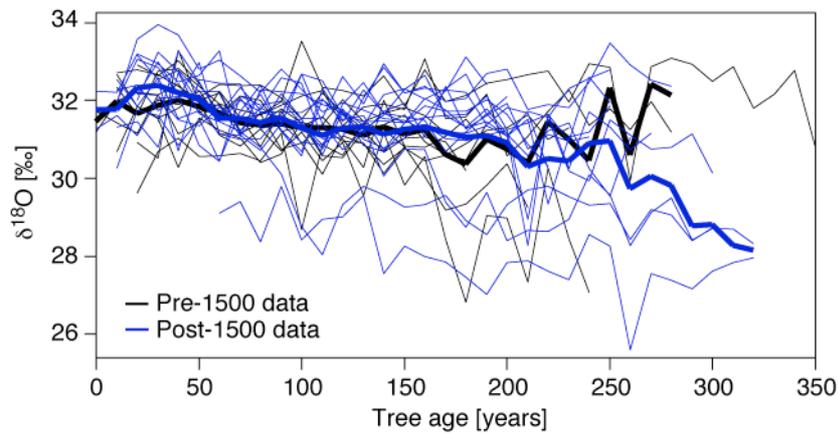
Parameter Coherence

Correlations between the detrended timeseries for each tree indicate varying coherences between parameter pairs. Figure A6 shows that all 25 δ^{18}O *vs.* TRW, and 19 MXD *vs.* TRW timeseries correlate positively. Coherence between δ^{18}O and MXD appears less significant, but also these parameters correlate positively in 21 trees. Note that the majority of correlations are insignificant though. Correlations between the other parameter pairs (δ^{18}O *vs.* δ^{13}C, δ^{13}C *vs.* MXD, δ^{13}C *vs.* TRW) are more balanced, i.e. both positive and negative associations are found, suggesting that these parameters are less dependent. To avoid age-trend influences, correlations were calculated using NegExp and Hug detrended timeseries (see Figure A5)

Figure A6. Tree-by-tree parameter correlations. Histogram shows the correlation coefficients between the NegExp (δ^{18}O, δ^{13}C, TRW) and Hug (MXD) detrended parameter timeseries for each of the 25 trees from the Pyrenees. Correlations are ordered from positive to negative. Bars on the right are the arithmetic means of the individual correlations.
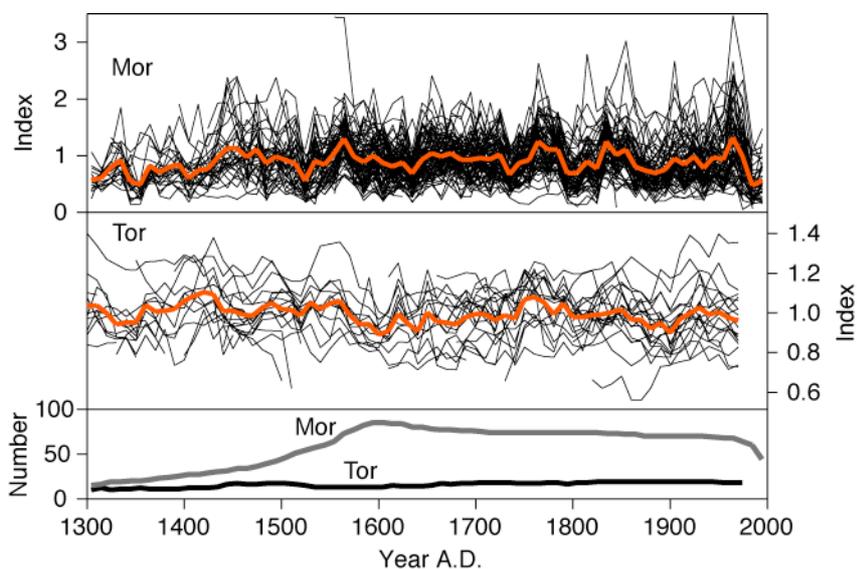
Lowest Frequency Oxygen Trends

To assess potential lowest frequency trends in tree-ring oxygen data, the δ^{18}O timeseries were split into pre- and post-1500 measurements – after truncation of some data bridging over the A.D. 1500 date line. This approach divides the dataset into 10 timeseries dating before and 15 timeseries dating after 1500. The individual measurement series and arithmetic means of the pre- and post-1500 subsamples are shown in Figure A7, after aligning the data by biological age. The match between the early and late subsamples suggest that there is no underlying lowest frequency trend in the tree-ring oxygen data, which could affect the assessment of age-related biases in this parameter.

Figure A7. Early-versus-late δ^{18}O data. A comparison of pre-1500 (in black) and post-1500 (blue) oxygen data is shown. All timeseries are aligned by tree age considering pith offset and data truncation. Thin curves represent decadal data from individual trees (10 pre-1500, 15 post-1500), bold curves are arithmetic means of these samples.

Moroccan and Swedish Data

To benchmark the isotope data from the Pyrenees, the records are compared with widely recognized TRW and MXD data from lake Tornetraesk in Northern Sweden [Grudd et al., 2002] and the Atlas Mountains in Morocco [Esper et al., 2007; Trouet et al., 2009]. Resolution of these data has been changed from annual to decadal, and coherence estimated using interseries-correlations (see main text). We here show the detrended 87 *Cedrus atlantica* series from Morocco together with 65 *Pinus sylvestris* series from Sweden (Figure A7). The Swedish pine data is on average shorter (mean series length is 300 years) than the Moroccan cedar data (480 years), but cover an overall longer period (441-1980 as compared to 1177-2001).

Figure A8. Decadally resolved Morocco TRW and Tornetraesk MXD data. Top and middle panels show the standardized TRW and MXD measurement series (in black) from the Atlas Mountains in Morocco and Lake Tornetraesk area in Sweden. Red curves are arithmetic means. Data were normalized [Mor, see Esper et al., 2007], and RCS detrended [Tor, see Grudd et al., 2002]. Bottom panel shows the replication curves of the data.

10

Table A1 Compilation of existing long-term (>300 years) $\delta^{18}O$ and $\delta^{13}C$ records. "Method" indicates whether single trees were processed individually, or after pooling wood samples prior to mass spectrometry.

Source	Parameter	Country	Species	Period	Number of trees	Max/min replication	Wood sample	Reso-lution	Method
Buhay & Edwards 1995	$\delta^{18}O$, δD	Canada	Ulmus americana, Pinus strobus, Acer saccharum	1610-1990	3	3/1	whole ring	decadal	individual
Buhay et al. 2008	$\delta^{13}C$	Canada	Picea glauca	1688-2003	2	2/1	whole ring	annual	individual
Edwards et al. 2008	$\delta^{13}C$, $\delta^{18}O$	Canada		951-1990	>16	9/1	whole ring	decadal	individual
Epstein & Krishna-murthy 1990	$\delta^{18}O$, δD	California	Pinus aristata	990-1950	1	1	whole ring	5-years	individual
Etien et al. 2008	$\delta^{13}C$, $\delta^{18}O$	France		1596-2000	?	?/3	latewood	annual	pooled
Freyer & Belacy 1983	$\delta^{13}C$	Germany	Quercus robur	1510-1950	5	5/1	whole ring	decadal	individual
Freyer & Belacy 1983	$\delta^{13}C$	Sweden	Pinus sylvestris	1480-1979	5	5/1	whole ring	decadal	individual
Gagen et al. 2007	$\delta^{13}C$	Finland	Pinus sylvestris	1612-2002	10	10/1	latewood	annual	individual
Kirdyanov et al. 2008	$\delta^{13}C$	Russia	Larix cajanderi	1588-2000	4	4/1	whole ring	annual	individual
Kitagawa & Matsu-moto 1995	$\delta^{13}C$	Japan	Cryptomeria japonica	124-1970	1	1	whole ring	decadal	individual
Krishnamurthy 1996	$\delta^{13}C$	Israel	Juniperus phoenica	1550-1950	1	1	whole ring	5-years	individual
Libby et al. 1976	$\delta^{18}O$	Germany	Quercus petrea	1350-1950	1	1	whole ring	3-4years	individual
Lipp et al. 1991	$\delta^{18}O$, δD	Germany	Abie alba	1004-1980	19	2/1	latewood	annual	individual
Stuiver & Braziu-mas 1987	$\delta^{13}C$	USA	Conifers	1100-1850	18	17/3	whole ring	decadal	individual
Treydte et al. 2006	$\delta^{18}O$	Pakistan	Juniperus turcestanica	951-1998	7	7/3	whole ring	annual	pooled & individual
Treydte et al. 2009	$\delta^{13}C$	Pakistan	Juniperus turcestanica	951-1998	7	7/3	whole ring	annual	pooled & individual
Isonet records									
Hilasvuori et al. 2009	$\delta^{13}C$, $\delta^{18}O$	Finland	Pinus sylvestris	1600-2002	4	4/2	whole ring	annual	pooled
Hilasvuori et al. 2009	$\delta^{13}C$, $\delta^{18}O$	Finland	Pinus sylvestris	1600-2002	4	4/2	whole ring	annual	pooled
Kress et al. 2009	$\delta^{13}C$, $\delta^{18}O$	Switzerland	Larix decidua	1650-2004	5	5/5	whole ring	annual	pooled & individual
Masson-Delmotte et al. 2005	$\delta^{13}C$, $\delta^{18}O$	France	Quercus robur	1611-1998	21	10/1	latewood	annual	pooled
Reynolds-Henne et al. 2007	$\delta^{13}C$, $\delta^{18}O$	Switzerland	Quercus petrea Pinus sylvestris	1637-2002	4	4/4	whole ring	annual	pooled & individual
Reynolds-Henne et al. 2007	$\delta^{13}C$, $\delta^{18}O$	Switzerland	Pinus sylvestris	1675-2003	4	4/4	whole ring	annual	pooled & individual
Rinne et al. 2009	$\delta^{13}C$, $\delta^{18}O$	UK	Quercus robur Pinus sylvestris	1604-2003	4	4/1	latewood	annual	pooled
Isonet records (not yet published)	$\delta^{13}C$, $\delta^{18}O$	Austria	Pinus nigra	1600-2002	4	?	whole ring	annual	pooled
	$\delta^{13}C$, $\delta^{18}O$	Austria	Quercus robur	1600-2003	4	?	latewood	annual	pooled
	$\delta^{13}C$, $\delta^{18}O$	Italy	Pinus leucodermis	1604-2003	4	?	whole ring	annual	pooled
	$\delta^{13}C$, $\delta^{18}O$	Morocco	Cedrus atlantica	1600-2000	4	?	whole ring	annual	pooled
	$\delta^{13}C$, $\delta^{18}O$	Norway	Pinus sylvestris	1600-2003	4	?	whole ring	annual	pooled
	$\delta^{13}C$, $\delta^{18}O$	Poland	Quercus robur	1627-2003	4	?	latewood	annual	pooled
	$\delta^{13}C$, $\delta^{18}O$	Spain	Pinus sylvestris	1600-2002	4	?	whole ring	annual	pooled
	$\delta^{13}C$, $\delta^{18}O$	Spain	Pinus uncinata	1600-2003	4	?	whole ring	annual	pooled
	$\delta^{13}C$, $\delta^{18}O$	Spain	Pinus nigra	1600-2002	4	?	whole ring	annual	pooled
Millennium records (in progress)	$\delta^{13}C$, $\delta^{18}O$ from 11 additional sites in Europe (10 conifer and 1 broadleaf). 9 of these are based on whole ring and 2 on latewood samples (1 conifer and 1 broadleaf).								

References

Büntgen, U. D. C. Frank, H. Grudd, and J. Esper (2008), Long-term summer temperature variations in the Pyrenees. *Clim. Dyn., 31*, 615–631.

Buhay, W.M., and T.W.D. Edwards (1995), Climate in southwestern Ontario, Canada, between AD 1610 and 1885 inferred from oxygen and hydrogen isotopic measurements of wood cellulose from trees in different hydrologic settings. *Quat. Res., 44*, 438–446.

Buhay, W.M., S. Timsic, D. Blair, J. Reynolds, S. Jarvis, D. Petrash, M. Rempel, and D. Bailey (2008), Riparian Influences on Carbon Isotopic Compositions of Tree-Rings in the Slave River Delta, Northwest Territories, Canada. *Chem. Geology, 252*, 9–20.

Cook, E. R. (1985), A Time Series Approach to Tree-Ring Standardization. *PhD Dissertation, University of Arizona*, Tucson, AZ, USA.

Edwards, T.W.D., S.J. Birks, B.H. Luckman, and G.M. MacDonald (2008), Climatic and hydrologic variability during the past millennium in the eastern Rocky Mountains and northern Great Plains of western Canada. *Quat. Res., 70*, 188–197.

Epstein, S., and R.V. Krishnamurthy (1990), Environmental information in the isotopic record in trees. *Philosoph. Transactions Royal Soc., 330A*, 427–439.

Esper, J., D. C. Frank, U. Büntgen, A. Verstege, J. Luterbacher, and E. Xoplaki (2007), Long-term drought severity variations in Morocco. *Geophys. Res. Lett., 34,* doi: 10.1029/2007GL030844.

Etien, N., V. Daux, V. Masson-Delmotte, M. Stievenard, V. Bernard, S. Durost, M.T. Guillemin, O. Mestre, and M. Pierre (2008), A bi-proxy reconstruction of Fontainebleau (France) growing season temperature from A.D. 1596 to 2000. *Clim. Past, 4*, 91–106.

Freyer, H.D., and N. Belacy (1983), $^{13}C/^{12}C$ records in Northern Hemispheric trees during the past 500 years: anthropogenic impact and climatic superpositions. *J Geophys. Res., 88*, 6844–6852.

Gagen, M., D. McCarroll, N.J. Loader, I. Robertson, R. Jalkanen, and K.J. Anchukaitis (2007), Exorcising the 'segment length curse': summer temperature reconstruction since AD 1640 using non-detrended stable carbon isotope ratios from pine trees in northern Finland. *Holocene, 17*, 435–446.

Grudd, H., K. R. Briffa, W. Karlén, T. S. Bartholin, P. D. Jones, and B. Kromer (2002) A 7400-year tree-ring chronology in northern Swedish Lapland: natural climatic variability expressed on annual to millennial timescales. *Holocene, 12*, 657–665.

Hilasvuori, E., F. Berninger, E. Sonninen, H. Tuomenvirta, and H. Jungner (2009), Stability of climate signal in carbon and oxygen isotope records and ring width from Scots pine (*Pinus sylvestris* L.) in Finland. *J. Quat. Science, 24*, 469–480.

Kirdyanov, A.V., K. Treydte, A. Nikolaev, G. Helle, and G.H. Schleser (2008), Climate signals in tree-ring width, density and $\delta^{13}C$ from larches in Eastern Siberia (Russia). *Chem. Geology, 252*, 31–41.

Kitagawa, H., and E. Matsumoto (1995), Climatic implications of $\delta^{13}C$ variations in a Japanese cedar (*Cryptomeria japonica*) during the last two millenia. *Geophys. Res. Lett., 22*, 2155–2158.

Kress, A., M. Saurer, U. Büntgen, K. Treydte, R.T.W. Siegwolf, H.K.M. Bugmann (2009), Summer temperature dependency of larch budmoth outbreaks revealed by Alpine tree-ring isotope chronologies. *Oecologia, 160*, 353–365.

Krishnamurthy, R.V. (1996), Implications of a 400 year tree ring based $^{13}C/^{12}C$ chronology. *Geophys. Res. Lett., 23*, 371–374.

Leuenberger, M. (2007), To what extent can ice core data contribute to the understanding of plant ecological developments of the past? In: T. E. Dawson, and R. T. W. Siegwolf, *Stable Isotopes as Indicators of Ecological Change*, Academic Press, London, pp. 211–233.

Libby, L.M., L.J. Pandolfi, P.H. Payton, III.J. Marshall, B. Becker, and V. Giertz-Siebenlist (1976), Isotopic tree thermometers. *Nature, 261*, 284–290.

Lipp, J., P. Trimborn, P. Fritz, H. Moser, B. Becker, and B. Frenzel (1991), Stable isotopes in tree ring cellulose and climatic change. *Tellus, 43B*, 322–330.

Masson-Delmotte V., Raffalli-Delerce G. P., Danis A., Yiou P.,Stievenard M., Guibal F., Mestre O., Bernard V., Goosse H., Hoffmann G. and Jouzel J. (2005), Changes in European precipitation seasonality and in drought frequencies revealed by a four-century-long tree-ring isotopic record from Brittany, western France. *Clim. Dyn., 24*, 57–69.

Reynolds-Henne, CE, R.T.W. Siegwolf, K. Treydte, J. Esper, S. Henne, and M. Saurer (2007), Temporal stability of climate-isotope relationships in tree rings of oak and pine (Ticino, Switzerland). *Glob. Biochem. Cycles, 21,* doi:10.1029/2007GB002945.

Rinne, K.T, N.J. Loader, V.R. Switsur, K. Treydte, and J.S. Waterhouse (2010), Investigating the influence of sulfur dioxide on the stable isotope ratios of tree rings. *Geochimica et Cosmochimica Acta, 74*, 2327–2339.

Suess, H. E. (1955), Radiocarbon concentration in modem wood. *Science, 122*, 415–417.

Stuiver, M., and T.F. Braziunas (1987), Tree cellulose ^{13}C/^{12}C isotope ratios and climate change. *Nature, 328*, 58–60.

Treydte, K., G.H. Schleser, G. Helle, D.C. Frank, M. Winiger, G.H. Haug, and J. Esper (2006), The twentieth century was the wettest period in northern Pakistan over the past millennium. *Nature, 440*, 1179–1182.

Treydte, K., D. C. Frank, M. Saurer, G. Helle, G. Schleser, and J. Esper (2009), Impact of climate and CO2 on a millennium-long tree-ring carbon isotope record. *Geochim. et Cosmochimica Acta, 73,* 4635–4647.

Trouet, V., J. Esper, N. E. Graham, A. Baker, J. D. Scourse, and D. C. Frank (2009), Persistent positive North Atlantic Oscillation mode dominated the Medieval Climate Anomaly. *Science, 324*, 78–80.